Chemistry & Biology
Article

Natural Product-Like Macrocyclic *N*-Methyl-Peptide Inhibitors against a Ubiquitin Ligase Uncovered from a Ribosome-Expressed De Novo Library

Yusuke Yamagishi,[1] Ikuo Shoji,[2] Shoji Miyagawa,[2] Takashi Kawakami,[1] Takayuki Katoh,[3] Yuki Goto,[3] and Hiroaki Suga[3,*]
[1]Department of Chemistry and Biotechnology, Graduate School of Engineering, The University of Tokyo, 7-3-1 Hongo, Bunkyo-ku, Tokyo 113-8656, Japan
[2]Division of Microbiology, Center for Infectious Diseases, Kobe University Graduate School of Medicine, 7-5-1 Kusunoki-cho, Chuo-ku, Kobe, Hyogo 650-0017, Japan
[3]Department of Chemistry, Graduate School of Science, The University of Tokyo, 7-3-1 Hongo, Bunkyo-ku, Tokyo 113-0033, Japan
*Correspondence: hsuga@chem.s.u-tokyo.ac.jp
DOI 10.1016/j.chembiol.2011.09.013

SUMMARY

Naturally occurring peptides often possess macrocyclic and *N*-methylated backbone. These features grant them structural rigidity, high affinity to targets, proteolytic resistance, and occasionally membrane permeability. Because such peptides are produced by either nonribosomal peptide synthetases or enzymatic posttranslational modifications, it is yet a formidable challenge in degenerating sequence or length and preparing libraries for screening bioactive molecules. Here, we report a new means of synthesizing a de novo library of "natural product-like" macrocyclic *N*-methyl-peptides using translation machinery under the reprogrammed genetic code, which is coupled with an in vitro display technique, referred to as RaPID (random nonstandard peptides integrated discovery) system. This system allows for rapid selection of strong binders against an arbitrarily chosen therapeutic target. Here, we have demonstrated the selection of anti-E6AP macrocyclic *N*-methyl-peptides, one of which strongly inhibits polyubiqutination of proteins such as p53.

INTRODUCTION

Peptides discovered as natural products share structural features that are not seen in ordinary polypeptides (proteins) expressed by the translation apparatus. Such "nonstandard" peptides are often macrocyclized and *N*-methylated in the backbone (Chatterjee et al., 2008); moreover, some of their side chains are modified to noncanonical functional groups or epimerized to *D*-configuration (Grünewald and Marahiel, 2006; Kohli et al., 2002; Li and Roller, 2002). These features concede critical biological and pharmacological properties, such as high affinity to binding partners, proteolytic resistance, and membrane permeability, and thus increase their specific potencies in vivo (Biron et al., 2008; Doedens et al., 2010; Driggers et al., 2008; Nestor, 2009; Sagan et al., 2004). Most of these peptides are produced by nonribosomal peptide synthetases (Grünewald and Marahiel, 2006; Kohli et al., 2002; Li and Roller, 2002) or are derived from ribosomally expressed peptides by enzymatic posttranslational modifications (Chatterjee et al., 2005; McIntosh et al., 2009; Oman and van der Donk, 2010). Despite the fact that libraries of "natural product-like" nonstandard peptides could be a very attractive source for drug discovery campaigns, the mechanistic and functional complexities of their production systems have been making it difficult for researchers to degenerate the sequences and lengths of nonstandard peptides and build their de novo library. Therefore, we have not yet witnessed a successful outcome of the generation of a highly complex "human-made" library and the discovery of novel peptide sequences against therapeutic targets.

Here, we report a unique means of synthesizing a "natural product-like" peptide library using a custom-made translation apparatus under the reprogrammed genetic code. The peptides in the library have the features of macrocyclic and *N*-methylated backbone along with a *D*-amino acid involvement in the sequences. Moreover, the library could be coupled with an in vitro display, and thus over a trillion members of nonstandard peptides can be rapidly screened against a chosen target. We referred to this platform system as RaPID (random nonstandard peptides integrated discovery) system. As a showcase of this system, we have performed selection of anti-E6AP macrocyclic *N*-methyl-peptides, and one of the abundant classes of selected peptides exhibited an inhibitory activity against E6AP-catalyzed polyubiquitination of target proteins, such as p53 and peroxiredoxin 1. Thus, the present work demonstrates a proof-of-technology and potentials of the RaPID system for the discovery of a novel class of nonstandard peptides against not only an E3 Ubquitin ligase but also previously nondruggable target families.

RESULTS AND DISCUSSION

Design of a Nonstandard Peptide Library Used in the RaPID System

The methodology of genetic code reprogramming, where arbitrary codons are reassigned from proteinogenic amino acids to nonproteinogenic amino acids, allows us to express "nonstandard" peptides using a translation apparatus (Forster et al., 2003; Josephson et al., 2005; Ohta et al., 2007; Ohta et al., 2008). To facilitate such a reprogramming, we have

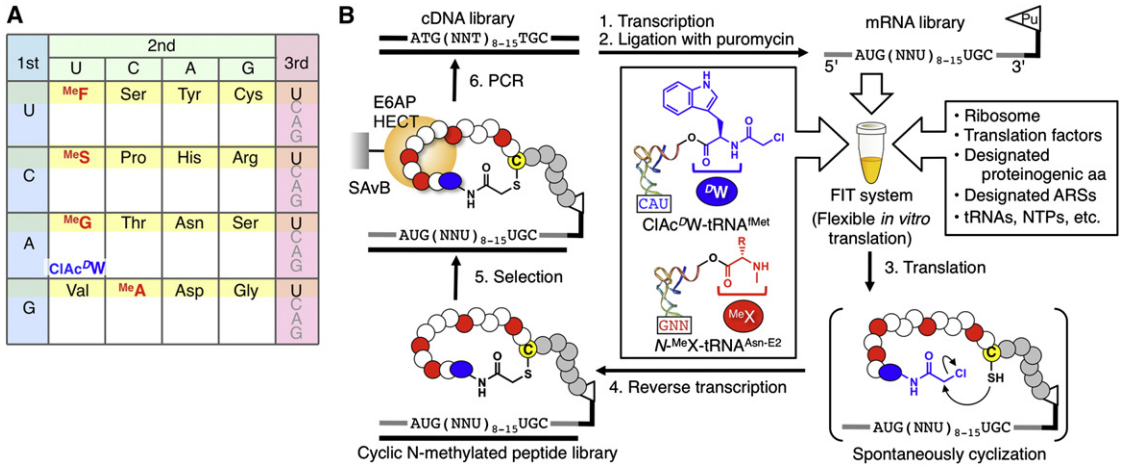

Figure 1. In Vitro Selection of Macrocyclic *N*-Methylated Peptides against E6AP HECT Domain by RaPID System

(A) The genetic code reprogrammed for this study. Four *N*-methyl-amino acids (^{Me}F, ^{Me}S, ^{Me}A, and ^{Me}G) and chloroacetyl-*D*-tryptophan (ClAc^{D}W) are shown in red and blue, respectively.

(B) Overview of the RaPID system for the selection of macrocyclic *N*-methyl-peptides. Messenger RNA libraries containing random sequence domain, $(NNU)_{8-15}$, were transcribed from the corresponding cDNA library and were conjugated with an oligonucleotide bearing a 3′-puromycin residue. The resulting mRNAs were translated by FIT system in the presence of the appropriate aminoacyl-tRNAs prepared by flexizymes. Linear peptides displayed on the individual mRNAs were spontaneously cyclized after translation, and the resulting macrocyclic peptides are displayed. The peptide libraries were then subjected to biotin-Avi-$(His)_6$-GB1-HECT immobilized on streptavidin magnetic beads (SAvB), and active species are isolated. Reverse transcription was performed after the selection in the first round and before the selection from the second round. The cDNAs on active mRNA-peptide fusion were recovered and amplified by PCR.

developed the FIT (flexible in-vitro translation) system (Goto et al., 2011). This system involves a custom-made *Escherichia coli* reconstituted cell-free translation system (Kung et al., 1977; Shimizu et al., 2001), where arbitrary amino acids and cognate aminoacyl-tRNA synthetases (ARSs) can be omitted to make the corresponding codons vacant, to which nonproteinogenic amino acids are assigned by supplementing the corresponding aminoacyl-tRNAs prepared by the flexizyme (flexible tRNA acylation ribozyme) technology (Murakami et al., 2006; Ohuchi et al., 2007). In fact, by using a customized FIT system, we were able to express macrocyclic *N*-methyl-peptides under the genetic code reprogrammed with more than four kinds of *N*-methyl-amino acids (Kawakami et al., 2008). To construct highly diverse libraries of nonstandard peptides and to effectively screen them for designated bioactivity, the FIT system was further integrated with an in vitro display method, so-called mRNA display (Nemoto et al., 1997; Roberts and Szostak, 1997). By this integration, nonstandard peptides expressed by the FIT system would be covalently ligated to the respective mRNAs via puromycin, displaying nonstandard peptides for the desired activity panning. We referred this mRNA display system integrated with FIT system to as RaPID (random nonstandard peptides integrated discovery) system.

In the present work, we assigned five nonproteinogenic amino acids, *N*-(2-chloroacetyl)-*D*-tryptophan (ClAc^{D}W), *N*-methylphenylalanine (^{Me}F), *N*-methylserine (^{Me}S), *N*-methylglycine (^{Me}G), and *N*-methylalanine (^{Me}A), to AUG, UUU, CUU, AUU, and GCU codons by the addition of ClAc^{D}W-tRNA$^{fMet}_{CAU}$, ^{Me}F-tRNA$^{Asn\text{-}E2}_{GAA}$, ^{Me}S-tRNA$^{Asn\text{-}E2}_{GAG}$, ^{Me}G-tRNA$^{Asn\text{-}E2}_{GAU}$, and ^{Me}A-tRNA$^{Asn\text{-}E2}_{GGC}$, respectively, prepared by the flexizyme technology (Figure 1A). A mRNA library was constructed to have NNU codon (N represents any of four bases, A, G, C, and U) with the mixture of repeats from eight to 15, $(NNU)_{8–15}$; thereby, *N*-methyl-amino acids would randomly appear in this region with the lengths of eight to 15 residues. In right downstream of the random region, UGC that assigns cysteine (Cys) was installed. Because all expressed peptides should have a ClAc^{D}W at the N terminus assigned by AUG start codon, the ClAc group would intramolecularly react with the sulfhydryl group of the Cys residue assigned by UGC or potentially UGU appeared in the random region, macrocyclizing their backbone via a nonreducible thioether bond (Goto et al., 2008; Kawakami et al., 2008). Following the UGC codon, three repeats of (GGC)(AGC) encoding $(Gly\text{-}Ser)_3$ followed by UAG stop codon are embedded. The 3′ common sequence would facilitate the display of macrocyclic *N*-methyl-peptides on the respective mRNA molecules via the $(Gly\text{-}Ser)_3$-puromycin linkage (Figure 1B).

Three critical notes should be given for securing a high quality of the macrocyclic *N*-methyl-peptide library: (1) In this FIT system, the amino acids and their cognate ARSs, whose codons were reprogrammed (F, L, I, and A), were omitted from the translation components, minimizing the unwanted incorporation of these proteinogenic amino acids competing with the *N*-methyl-amino acids. Similarly, those unassigned by NNU codons (Q, K, E, and W) were omitted. Moreover, release factor-1 (RF1) was withdrawn to aim at halting elongation at UAG codon and thus increasing the efficiency of puromycin-peptide fusion. (2) Because four of 16 codons assigned by the NNU mRNA library encode *N*-methyl-amino acids, one *N*-methyl-amino acid residue would appear in every four residues by chance. Our previous studies suggested the thioether macrocyclization takes place cleanly in nearly quantitative manner, regardless of the length and composition of peptide

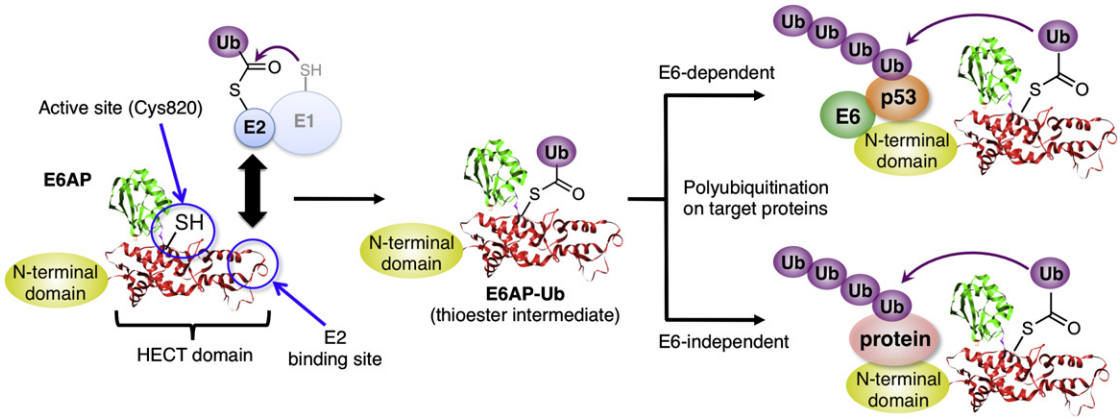

Figure 2. E6AP-Catalyzing Polyubiqutination of Target Proteins in E6-Independent and -Dependent Manners
In general, ubiquitin-activating enzyme E1 delivers an ubiquitin molecule (Ub) onto ubiquitin-conjugating enzyme E2 via a thioester linkage, and then Ub on E2 is transferred to ubiquitin ligase E3 forming a conjugate, E3-Ub. E6AP HECT (homologous to E6-associated protein [E6AP] C-terminus) domain (PDB 1C4Z), belonging to a member of E3 protein family, cooperatively catalyzes polyubiquitination on certain proteins, such as p53, with E6 (E6-dependent pathway) or directly polyubiquitinates various target proteins (E6-indendent pathway).

sequences (Goto et al., 2008; Kawakami et al., 2008). Moreover, because no stop codon was encoded in the $(NNU)_{8–15}$ random region, the highly reliable macrocyclic *N*-methyl-peptide library could be displayed by RaPID system. (3) The initial mRNA library consists of greater than 6×10^{12} unique members. It should be noted that the complexity of $(NNU)_{8–15}$ mRNA library should almost directly reflect to the peptide library complexity because only Ser is redundant in the genetic triplets used. Because the generally observed yield of mRNA-peptide fusion in the FIT system was 30% or more of the total input of mRNA, the diversity of the initial RaPID display library was estimated to be 10^{12} or more.

RaPID Selection against E6AP HECT Domain

The ubiquitin-proteasome system regulates the degradation of cellular proteins through enzyme cascade consisting of ubiquitin-activating enzyme E1, ubiquitin-conjugating enzyme E2, and ubiquitin (Ub) ligase E3 (Figure 2) (Hershko and Ciechanover, 1998; Pickart, 2001). Many families of E3 Ub ligases are known and are responsible for specific conjugation of polyubiquitins (polyUbs) to designated proteins, directing them to proteasome and thus triggering their proteolysis. Misregulation of the proteolysis of certain proteins caused by malfunction of E3 family ligases influences their downstream signal transduction processes, and therefore causes human disorders such as cancer (Hoeller et al., 2006) and neurodegeneration (Layfield et al., 2005; Rubinsztein, 2006). Thus, these E3 Ub ligases could be attractive targets for new therapeutic intervention (Eldridge and O'Brien, 2010; Hoeller and Dikic, 2009; Nalepa et al., 2006). Homologous to E6AP C-terminus (HECT) domain belongs to a family member of E3, and its N terminus domain cooperates with the human papillomavirus (HPV) E6 protein originating from the high-risk virus types 16 and 18 (Beaudenon and Huibregtse, 2008; Scheffner et al., 1993). The resulting E6AP and E6 complex provides the specific E3 ligase activity in the transfer of polyUbs onto p53 for the promotion of degradation, inhibiting p53-dependent apoptosis pathways (Figure 2). Moreover, it has been discovered that E6AP ubiquitinates some endogenous human proteins, such as HHR23A (a human homolog of the yeast DNA repair protein Rad23) (Kumar et al., 1999) and PML (promyelocytic leukemia) tumor suppressor (Louria-Hayon et al., 2009), in an E6-independent manner, suggesting that it also promotes the degradation of tumor-associated proteins. Despite advances in understanding of the molecular mechanism and structural study for HECT domains of E6AP (Huang et al., 1999) and other related enzymes (Eletr and Kuhlman, 2007; Ogunjimi et al., 2005), to the best of our knowledge, no selective inhibitor against E6AP has been yet reported by means of high-throughput screenings. Therefore, the development of inhibitors against HECT domain remains a formidable challenge. We here chose E6AP as a previously nondruggable target and performed selection of anti-E6AP peptides using RaPID system.

E6AP HECT domain was expressed as a fusion protein with an Avi-$(His)_6$-tag followed by a solubility-enhancement tag GB1 (streptococcal B1 immunoglobulin-binding domain of protein G) (Liu et al., 2009; Zhou et al., 2001) at the N terminus. This protein construct, Avi-$(His)_6$-GB1-HECT, in which Avi domain was biotinylated during the expression, was immobilized on streptavidin magnetic beads (SAvB, Figure 1B). The library was applied to the protein beads, and the bound fractions were selected at 4°C in the first and second round (Figure 3A). From the third round, GB1-immobilized SAvB was used as the negative selection to remove GB1-binding peptides, and then the positive selection was performed at 37°C to enrich the population with specific binding activity against the HECT domain. In the sixth round, we observed a significant increase in recovery rate of active fractions (Figure 3A), and therefore the resulting cDNA sequences in the pool were analyzed.

The sequence alignment of 47 clones revealed eight independent sequence families found in the pool 6 (Figure 3B). Six families, CM_{11}-1–6, are originating from the $(NNU)_{11}$ pool, whereas the remaining two families, CM_{13}-7 and CM_{13}-8, are from the $(NNU)_{13}$ pool. The most abundant sequence, CM_{11}-1, bearing four *N*-methyl residues, shares several common signatures of

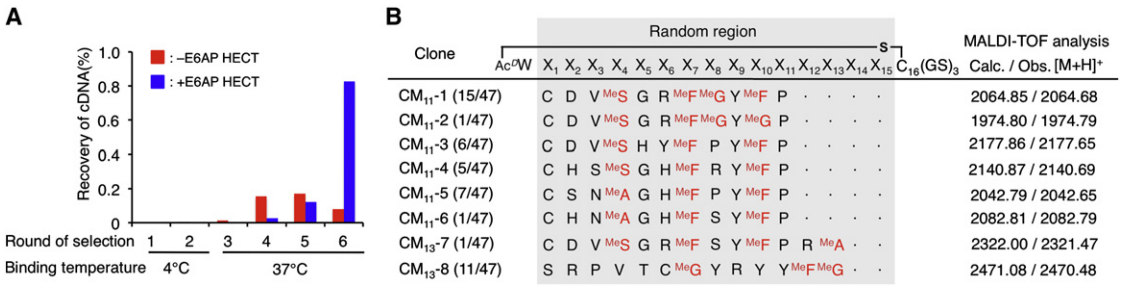

Figure 3. In Vitro Selection of Macrocyclic *N*-Methyl-Peptides against E6AP HECT Domain and Selected Active Species

(A) Progress of the selection. Recovery rates of cDNA from each round were estimated by recovered amounts over input amounts of cDNAs monitored by real-time PCR. The first and second rounds of selection were performed at 4°C, and the subsequent rounds were performed at 37°C. Those determined against SAvB•biotin-Avi-$(His)_6$-GB1-HECT as a positive selection are shown in blue, whereas those against SAvB•biotin-Avi-$(His)_6$-GB1 as a negative selection shown in red.

(B) Peptide sequences identified from the pool in round 6. The apparent frequency over a total number of clones and *N*-methyl amino acids of each sequence are shown in parentheses and red, respectively. The parental random region is highlighted in gray, in which a dot denotes a residue that did not appear in the random X_{12-15} region. Calculated (Calc.) and observed (Obs.) mass values ($[M+H]^+$) of each peptide expressed by FIT system are shown. See also Figure S1 and Table S1.

residues with other sequences. $^{Me}S_4$, G_5, $^{Me}F_7$, Y_9, $^{Me}F_{10}$, and P_{11} are highly conserved in CM_{11}-1–6 and CM_{13}-7, where four residues are notably the secondary amino acids. Among them, $^{Me}F_{10} \rightarrow {}^{Me}G_{10}$ as well as $^{Me}S_4 \rightarrow {}^{Me}A_4$ substitutions were found in CM_{11}-2 and CM_{11}-5/CM_{11}-6, respectively, suggesting that the role of side chain group may be less important in activity but critical to be the *N*-methyl substituent. Moreover, $^{Me}G_8$ could be substituted with P_8 observed in abundant CM_{11}-3 and CM_{11}-5, whereas another abundant CM_{11}-4 and two other independent peptides CM_{11}-6–7 have R_8 and S_8, respectively. This may suggest that X_8 prefers to be the secondary amino acid but tolerates other amino acid substitutions. Mutations occurred during the course of selection is discussed more details in the Supplemental Information (see Figure S1 available online).

It is intriguing that the selection yielded only two lengths of *N*-methyl-peptides from the $(NNU)_{8-15}$ random region, given that other lengths of peptides should coexist in the initial pool, suggesting that the three-dimensional structure arisen from these two lengths might be critical to exhibit binding activity against E6AP HECT domain (Figure 3B). Importantly, the successful outcomes clearly demonstrated that the *N*-methyl-peptide library used in this study had a reliable quality and high complexity giving the *N*-methyl residues in the random region, and the RaPID system enabled us to select active species effectively and rapidly. The observed similarity in the composition of amino acid residues, particularly the positions as well as kinds of *N*-methyl residues appeared in the sequences, also suggests that specific interactions between the selected *N*-methyl-peptides and E6AP HECT domain are very likely occurring.

Characterization of Isolated Anti-E6AP Macrocyclic *N*-Methyl-Peptides

To confirm whether the identified mRNA sequences of CM_{11}-1–6 and CM_{13}-7–8 correctly produced the encoding macrocyclic *N*-methyl-peptides, we constructed the respective mRNA templates with a substitution of UAG with UAA that acts as a terminator of endogenous RF2 and performed in vitro expression using the same FIT system as the selection (Figure 3B, data in the column of MALDI-TOF analysis). MALDI-TOF analysis of the crude product expressed from the respective mRNA template showed a clean peak of which molecular mass is consistent with that calculated. This observation made us confident that the selected peptides had the *N*-methylated backbone as well as the composition of residues, as we expected from the cDNA sequences. For further characterization, we decided to focus on three abundant peptides, CM_{11}-1, CM_{11}-3, and CM_{11}-5, all of which consist of a total of 14 amino acid residues. The respective *N*-methyl-peptides were chemically synthesized by standard Fmoc solid-phase chemistry where the C terminus of G_{17} (corresponding to the 14th residue) was modified with carboxyamide (Table S1).

Because the above three peptides have a cysteine residue at position 1 (C_1) in the random region adjacent to $ClAc^DW$, cyclization between the ClAc group with C_1 side chain designated by UGU would potentially compete with that between the ClAc group with C_{16} side chain designated by UGC. To decipher which cyclization preferentially or selectively occurred, we synthesized three peptides based on CM_{11}-1 as a representative peptide; one is CM_{11}-1 itself, and the others are $C_1 \rightarrow S_1$ mutant of CM_{11}-1 (CM_{11}-1S_1) and the corresponding to linear *N*-methyl-peptide by altering ClAc to acetyl (Ac) group, referred to as LM_{11}-1 (Table 1). Fragmentation of LM_{11}-1 by MALDI-TOF/TOF yielded peaks corresponding to linear fragments, as expected (Figure S2A). On the other hand, MALDI-TOF/TOF fragmentation of CM_{11}-1 and CM_{11}-1S_1 was much difficult than that for LM_{11}-1, and both gave similar fragmentation patterns (Figures S2B and S2C). Importantly, we were able to identify peaks corresponding to fragments containing the thioether linkage between the N-terminal acetyl group and the sulfhydryl group of C_{16} side chain in both CM_{11}-1 and CM_{11}-1S_1, but not between Ac and C_1 side chain in CM_{11}-1. These results well agree with the selective formation of the thioether linkage of Ac-S-C_{16}.

To evaluate the binding abilities of chosen peptides, CM_{11}-1, CM_{11}-3, and CM_{11}-5 (a series of these peptides are referred to as CM_{11}-peptides), we determined their kinetic and dissociation constants by means of surface plasmon resonance (SPR)

Table 1. Kinetic and Equilibrium Constants of Macrocyclic *N*-Methyl-Peptides against E6AP HECT Domain

Peptide	Sequence	k_{on} (x10^6) $M^{-1}s^{-1}$	k_{off} (x10^{-3}) s^{-1}	K_d nM
CM_{11}-1	Ac^{D}WCDV^{Me}SGR^{Me}F^{Me}GY^{Me}FPCG-NH_2 (S–C)	2.66	1.60	0.60
LM_{11}-1	Ac^{D}WCDV^{Me}SGR^{Me}F^{Me}GY^{Me}FPCG-NH_2	0.047	8.46	180
CM_{11}-1S_1	Ac^{D}WSDV^{Me}SGR^{Me}F^{Me}GY^{Me}FPCG-NH_2 (S–C)	1.33	15.5	11.7
CP_{11}-1	Ac^{D}WCDV S GR F G Y F PCG-NH_2 (S–C)	not detectable		>1000
LP_{11}-1	Ac^{D}WCDV S GR F G Y F PCG-NH_2	not detectable		>1000
CM_{11}-3	Ac^{D}WCDV^{Me}SHY^{Me}F P Y ^{Me}FPCG-NH_2 (S–C)	0.257	0.320	1.24
LM_{11}-3	Ac^{D}WCDV^{Me}SHY^{Me}F P Y^{Me}FPCG-NH_2	0.014	4.46	325
CM_{11}-5	Ac^{D}WCSN^{Me}AGH^{Me}F P Y^{Me}FPCG-NH_2 (S–C)	2.19	2.87	1.31
LM_{11}-5	Ac^{D}WCSN^{Me}AGH^{Me}F P Y^{Me}FPCG-NH_2	0.089	20.6	231

Data were collected by the standard SPR method using Biocore T100 and the constants were generated by the equipped data fitting program. See also Figures S2 and S3.

analysis against the E6AP Avi-$(His)_6$-GB1-HECT domain immobilized on a SAv-sensor chip (Table 1). All macrocyclic CM_{11}-peptides have values of k_{on} with a range of 0.2–3 × 10^6 $M^{-1}s^{-1}$, k_{off} with a range of 0.3–3 × 10^{-3} s^{-1}, resulting in the dissociation constants (K_d) with subnanomolar to 1 nM range. Thus, the representative CM_{11}-peptides studied here have remarkably strong affinity to E6AP HECT domain, and particularly CM_{11}-1 has the lowest K_d values among the CM_{11}-peptides. In addition to the CM_{11}-peptides, we synthesized the respective linear peptides bearing N-terminal acetyl group, referred to as LM_{11}-peptides. All LM_{11}-peptides lost affinity over 170-fold. This suggests that the macrocyclic structure closed by the Ac-S-C_{16} thioether bond in CM_{11}-peptides is crucial to exhibit high binding activity to the HECT domain.

In addition to the above peptides, we synthesized three more mutants of CM_{11}-1 to further validate the importance of the specific structure. One was the aforementioned $C_1 \rightarrow S_1$ mutant peptide, CM_{11}-1S_1, and the others are a macrocyclic peptide without N-methyl backbone but having the same side chains, CP_{11}-1, and its linear peptide, LP_{11}-1 (Table 1). CM_{11}-1S_1 had a 9-fold faster k_{off} rate than CM_{11}-1, implying that C_1 somehow contributes to slowing the dissociation from the target site but is not absolutely essential for binding activity. On the other hand, the other two mutants completely lost binding ability, indicating that *N*-methylated backbone with the N-terminal Ac-C_{16} thioether macrocycle is crucial to maintain the full binding capability of CM_{11}-1 against E6AP HECT domain.

Furthermore, we verified the binding specificity of CM_{11}-peptides against E6AP HECT domain using a different HECT-type E3 Ub ligase, Smurf2 (Ogunjimi et al., 2005). None of CM_{11}-peptides had any SPR signature of binding against Smurf2 Avi-$(His)_6$-GB1-HECT domain immobilized on a SAv-sensor chip, indicating that CM_{11}-peptides have high selectivity toward the E6AP HECT domain over Smurf2 HECT domain nor Avi-$(His)_6$-GB1-tag region (data not shown). Moreover, we investigated human plasma stability of CM_{11}-peptides compared with other control peptides (see more details in Supplemental Information and Figure S3), indicating that a CM_{11}-peptide (CM_{11}-1S_1) is very stable in plasma. Taken together, CM_{11}-peptides have remarkable binding activity and specificity to E6AP HECT domain and plasma stability.

CM_{11}-1 Inhibits Ubiquitination of Target Proteins Catalyzed by E6AP

Despite the observation of strong binding activity of CM_{11}-peptides to E6AP HECT domain, it does not necessarily mean that they are able to inhibit the E6AP ubiquitination activity. To assess whether CM_{11}-peptides have an ability to inhibit the ubiquitination activity, we chose the most active CM_{11}-1 and performed an in vitro assay to monitor ubiquitin thioester formation. It is known that E6AP or even its HECT domain alone forms the ubiquitin thioester intermediate (Beaudenon et al., 2005; Scheffner et al., 1990; Scheffner et al., 1995) in the presence of Ub, E1, and E2 in vitro (Figure 2). When an in vitro translation system from rabbit reticulocyte lysate (RRL), which contains these essential Ub-related components, was used for translating the E6AP HECT domain from the appropriate mRNA template in the presence of [^{35}S]-Met (Huibregtse et al., 1995),

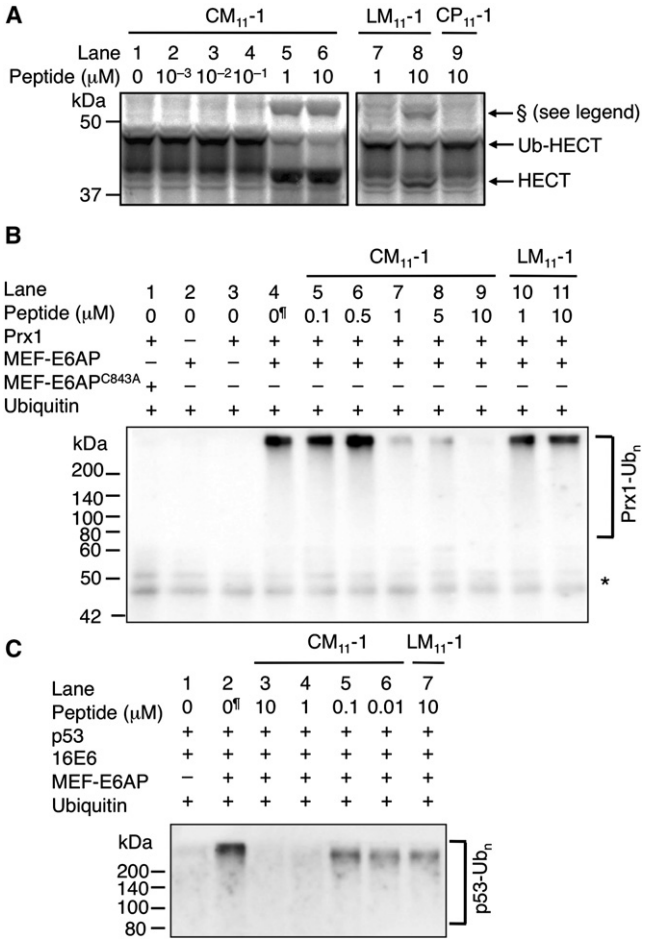

Figure 4. Inhibition of Ub-Thioester Formation with E6AP HECT Domain and Polyubiqutination of Target Proteins by CM_{11}-1 and Its Derivatives

(A) Inhibition of Ub-thioester formation with E6AP HECT domain. ^{35}S-labeled E6AP HECT (43 kDa) was translated in a rabbit reticulocyte lysate cell-free translation system. Because the translation lysate supposedly contained ubiquitin (8 kDa), E1, and E2, the expressed E6AP HECT would be endogenously converted to the ubiquitin-adduct (E6AP HECT-Ub, 51 kDa). The translation mixture was treated with various concentrations of peptides (10^{-3}–10 μM) at room temperature for 30 min. The resulting mixtures were analyzed by SDS-PAGE without DTT. §When the Ub-thioester formation on E6AP was inhibited by CM_{11}-1 (as well as 10 μM LM_{11}-1), a slower migrating band than Ub-E6AP appeared on the gel. Although the product of this band has not yet been defined, this band disappeared upon addition of a free thiol reagent such as DTT (data not shown), suggesting a possibility of dimer formation of HECT domain via a disulfide bond. Alternatively, the free cysteine in HECT domain formed a disulfide bond with other proteins containing a free cysteine residue.

(B) Inhibition of E6-independent polyubiquitination on Prx1. $(His)_6$-Prx1 was incubated with 250 nM MEF-E6AP or inactive mutant MEF-E6AP^{C843A}, $(His)_6$-E1, $(His)_6$-UbcH7, ubiquitin and peptide at 37°C for 30 min. Reaction products were immunoprecipitated with anti-Prx1 pAb and visualized by antiubiquitin mAb immunoblotting. Asterisk denotes immunoglobulin heavy chain. ¶As a negative control, DMSO used as a cosolvent for CM_{11}-1 inhibition was added.

(C) Inhibition of E6-dependent polyubiquitination on p53. p53 was incubated with 170 nM MEF-E6AP, $(His)_6$-E1, $(His)_6$-UbcH7, ubiquitin, HPV16 E6, and peptide at 37°C for 30 min. Reaction products were immunoprecipitated with anti-p53 pAb and visualized by antiubiquitin mAb immunoblotting. See also Figure S4.

a Ub-thioester intermediate of the ^{35}S-Met-labeled HECT domain (Ub-HECT) was distinguished from the parental HECT domain by means of a SDS-PAGE mobility shift assay (Figure 4A, lane 1). When CM_{11}-1 was added to this translation assay system, the migration shift was suppressed at 1 μM or higher concentrations (lanes 5 and 6). As a negative control, LM_{11}-1 and CP_{11}-1 were also tested for the same inhibition assay, in which an approximately 50% inhibition was observed at 10 μM LM_{11}-1, whereas neither 1 μM LM_{11}-1 nor 10 μM CP_{11}-1 exhibited the inhibition. Although the observed potency by CM_{11}-1 seemed not as strong as expected from the SPR data, this could be attributed to that the RRL translation system might contain endogenous label-free E6AP (Huibregtse et al., 1991; Scheffner et al., 1993) that might interact with some fractions of CM_{11}-1, resulting in a reduction of the apparent inhibitory potency. Nevertheless, this result suggests that CM_{11}-1 is able to inhibit the charge of Ub onto the HECT domain of E6AP.

We then have further pursued testing inhibition of E6AP-catalyzed polyubiquitination on target proteins. Peroxiredoxin 1 (Prx1) is an endogenous substrate of E6AP in human cells, and its polyubiquitination occurs independently from the presence of E6 (Nasu et al., 2010). To monitor the inhibitory action of CM_{11}-1 against E6AP, we used an in vitro-reconstituted Prx1 polyubiquitination assay system, in which purified His-tagged Prx1 was incubated with E6AP tagged with MEF (Myc-TEV protease site-flag) and ubiquitin in the presence of purified His-tagged E1 and E2 (UbcH7). The resulting polyubiquitinated Prx1 (Prx1-Ub_n) and free Prx1 were immunoprecipitated by anti-Prx1 polyclonal antibodies and were immunoblotted by an anti-Ub monoclonal antibody to visualize in SDS-PAGE (Figure 4B, lanes 1–9). As negative controls, LM_{11}-1 and CP_{11}-1 were also included in this examination. Clearly, polyubiquitination of Prx1 was inhibited by CM_{11}-1 in a dose-dependent manner (lanes 5–9), where an approximately 1 μM of CM_{11}-1 nearly shut down the E6AP activity. On the other hand, neither LM_{11}-1 (lanes 10 and 11) nor CP_{11}-1 (data not shown) was able to inhibit polyubiquitination. We also tested Prx1-polyubiquitination inhibition by CM_{11}-1S_1, showing a weaker inhibitory activity than CM_{11}-1 (Figure S4); the result seemed consistent with the K_d values for both peptides observed in SPR experiments.

Finally, we examined the inhibitory activity of CM_{11}-1 against polyubiquitination on an E6-dependent substrate, p53, using a reconstituted p53 polyubiquitination assay system. Immunoprecipitation of poly- and nonubiquitinated p53 using anti-p53 pAb followed by immunobolotting using anti-Ub mAb enabled us to detect the polyUb-p53 on SDS-PAGE (Figure 4C). Again, 1 μM CM_{11}-1 was able to inhibit polyubiquitination of p53 in a dose-dependent manner (lanes 3–6), whereas the control peptide, LM_{11}-1, was not (lane 7). The result shows that CM_{11}-1 acts as an E6AP inhibitor that prevents polyubiquitination of Prx1 and p53 in E6-independent and E6-dependent manner, respectively. The trend of K_d values of CM_{11}-1 and its mutant peptides against E6AP HECT domain determined by the SPR experiments well reflected to their observed inhibitory behaviors against ubiquitination of target substrates (Table 1 and Figure 4). Because the present assay method allowed us to detect polyubiquitination instead of monoubiquitination of the substrate proteins catalyzed by an excess amount of E6AP (greater than

two orders of magnitude) over the inherent K_d value of CM_{11}-1, the observed inhibitory potency of CM_{11}-1 was only qualitatively assessed. Most importantly, CM_{11}-1 was capable of inhibiting Ub ligase activity of E6AP even though it was simply selected by binding to E6AP.

SIGNIFICANCE

Here, we have demonstrated RaPID selection of "natural product-like" peptides consisting of thioether-macrocyclic and N-methylated backbone. The selection against E6AP HECT domain has yielded such desired peptides with remarkable binding abilities, falling in a range of K_d values from a subnanomolar to a single-digit nanomolar. One of the representative peptides, CM_{11}-1, chosen for further studies has displayed inhibitory activity against E6AP-catalyzing polyubiquitination on the target proteins, Prx1 and p53. The present work provides the proof-of-technology of RaPID system that enables for the discovery of potent inhibitors against a previously nondruggable ubiquitin ligase, thus opening a wide range of possibilities in the discovery of inhibitors against other ubiquitin ligase families. Most importantly, the natural product-like macrocyclic *N*-methyl-peptides have larger interaction surfaces compared with small organic molecules, as well as elevated stability under physiological conditions compared with ordinary peptides; therefore, they would provide tremendous potentials for the development of drug leads that disrupt not only enzyme activities but also protein-protein interactions.

EXPERIMENTAL PROCEDURES

In Vitro Translation and Selection

Translation of the first round selection was performed using 100 pmol mRNA-puromycin (initial complexity is 6×10^{13}) and 150 μl of translation mixture in the presence of 3750 pmol of ClAc^{D}W-tRNA$^{fMet}_{CAU}$, ^{Me}G-tRNA$^{Asn\text{-}E2}_{GAU}$, ^{Me}A-tRNA$^{Asn\text{-}E2}_{GGC}$, ^{Me}S-tRNA$^{Asn\text{-}E2}_{GAG}$, and ^{Me}F-tRNA$^{Asn\text{-}E2}_{GAA}$ (25 μM each), at 37°C for 30 min. Subsequently, the translation mixture was incubated at room temperature for 12 min to conjugate the translated peptide with the corresponding mRNA-puromycin. This solution was incubation with 15 μl of 200 mM EDTA (pH 8.0) at 37°C for 30 min in order to dissociate ribosomes from mRNA-peptide complexes. For the first-round selection, 11 μl of E6AP HECT immobilized streptavidin magnetic beads (Dynabeads M-280, Invitrogen) was used at a concentration of 200 nM target protein, and mixed with the solution of mRNA-displayed *N*-methyl-peptides. The binding reaction was performed at 4°C for 30 min with rotation. After supernatant was removed, the bead was washed with 300 μl of cold wash buffer (100 mM Tris-HCl [pH 7.5], 300 mM NaCl, 0.05% [v/v] tween 20). To the bead was added 40 μl of RT reaction buffer (50 mM Tris-HCl [pH 8.3], 75 mM KCl, 3 mM $MgCl_2$, 10 μM DTT, 0.5 mM dNTPs, 2 μM CGS3an13.R39) containing 200 units of M-MLV reverse transcriptase (Promega) and 8 units of RNase inhibitor (Promega), and reverse transcribed at 42°C for 60 min with rotation. The selected cDNA was eluted with 360 μl of PCR buffer (10 mM Tris-HCl [pH 7.5], 50 mM KCl, 0.1% [v/v] Triton X-100, 2.5 mM $MgCl_2$, 0.25 mM dNTPs, 0.25 μM T7g10M.F48, 0.25 μM CGS3an13.R39) at 95°C for 5 min. After addition of *Taq* DNA polymerase to the eluate, the mixture was used for PCR amplification. The amplified DNA was purified by the extraction with phenol/chloroform and ethanol purification and was used for the next round of selection. Since the second round, 10 μl scale of transcription and 7.5 μl of ligation with puromycin linker were carried out. The resulting mRNA-puromycin of the second round was translated using 5 μl of the translation mixture in the presence of each 25 μM acyl-tRNAs at 37°C for 30 min, followed by incubation at room temperature for 12 min. After incubation with 1 μl of 100 mM EDTA (pH 8.0) at 37°C for 30 min, the reverse transcription of the mRNA-displayed peptides was performed by RT reaction buffer in the presence of M-MLV reverse transcriptase without RNase H activity (Promega), at 42°C for 60 min with rotation. After quenching the reaction with 1 μl of 100 mM EDTA (pH 8.0), the solution was neutralized with 1.1 μl of 0.2 M HCl. The complexes with cDNA- and mRNA-displayed peptides were subjected to 2.4 μl of the magnetic bead without target and were incubated at 4°C for 30 min for negative selection at once. Subsequently, the supernatant was mixed with 0.8 μl of the magnetic bead with E6AP HECT and was incubated with 4°C for 30 min for positive selection, followed by thrice washing with 10 μl of cold wash buffer. After addition of 100 μl of PCR buffer to the bead, the cDNA were eluted at 95°C for 5 min and amplified by *Taq* DNA polymerase. In the third round and all subsequent rounds, the all experiments were performed by a half of the reaction scale of the second round. Moreover, negative selection was performed at 4°C for 20 min at three times in the third and fourth round, and at nine times in the fifth and sixth round. On the other hand, positive selections after second round were performed by mixing with the complexes of cDNA and mRNA-displayed peptides and 200 nM E6AP HECT (not immobilized on streptavidin magnetic bead) at 37°C for 30 min, followed by pull down by streptavidin magnetic bead at 37°C for 5 min with rotation. After thrice washing with 5 μl of wash buffer at room temperature, the selected cDNA was eluted with 100 μl of PCR buffer at 95°C for 5 min. After addition of *Taq* DNA polymerase to the eluate, the mixture was used for PCR amplification. To monitor the convergence of the selection process, real-time PCR (RT-PCR) was used to quantify the amounts of input and output DNA in every round. For input cDNA, 0.25 μl aliquot of the RT mixture was diluted with 150 μl of a dilution solution (10 mM Tris-HCl [pH 8.0] and 300 mM NaCl), and 1 μl of the diluted cDNA was mixed with 19 μl of PCR buffer containing SYBR Green I (Molecular Probe) and *Taq* DNA polymerase. For output cDNA, 1 μl aliquots of the eluates from the beads of positive and negative selections were mixed with 10 μl of PCR buffer containing SYBR Green I and *Taq* DNA polymerase. The reverse transcribed $(NNU)_{10}$ mRNA mixture was serial-diluted and used for the templates as standards.

MALDI-TOF Analysis of Translated Clone Peptides

To identify the expressed cyclic *N*-methylated peptides, a 5 μl scale translation reaction was performed using FIT system with 40 nM of clone DNA, 25 μM each of ClAc^{D}W-tRNA$^{fMet}_{CAU}$, ^{Me}G-tRNA$^{Asn\text{-}E2}_{GAU}$, ^{Me}A-tRNA$^{Asn\text{-}E2}_{GGC}$, ^{Me}S-tRNA$^{Asn\text{-}E2}_{GAG}$, and ^{Me}F-tRNA$^{Asn\text{-}E2}_{GAA}$ at 37°C for 30 min. After quenching with 0.2% TFA, the crude peptide mixture was desalted with C-Tip (C18 desalting SPE, Nikkyo technos) and eluted with 80% acetonitrile and 0.5% acetic acid solution saturated with the matrix α-cyano-4-hydroxycinnamic acid (Bruker Daltonics). MALDI-TOF analysis was performed using an Autoflex TOF/TOF (Bruker Daltonics) and peptide calibration standard II (Bruker Daltonics) as external standards.

SPR Analysis of Peptides

The interaction between E6AP HECT and peptides was assessed using a BIACORE T100 instrument (GE Healthcare) equipped with research-grade streptavidin sensor chip at 25°C. Biotinylated E6AP HECT was immobilized to a surface density of approximate 1,500 response units (RU) using standard immobilization protocols (GE Healthcare). HBS-EP+ (10 mM HEPES [pH 7.4], 150 mM NaCl, 3 mM EDTA, and 0.05% [v/v] surfactant P20) containing 1.0% (v/v) DMSO was used as the running buffer for all experiments. Peptide binding was tested by injecting varying concentrations (0.3 nM to 1,000 nM) at a flow rate of 30 μl min^{-1} and measured by single cycle kinetics method. Raw data were analyzed by the BIACORE T100 evaluation software 2.01 and fitted to the standard 1:1 interaction model.

In Vitro Ubiquitin Transfer Assay by ^{35}S-Labeled E6AP HECT

E6AP HECT cDNA was subcloned into pTNT vector (Promega) at XhoI and SalI sites. ^{35}S-Methionine-labeled E6AP HECT was synthesized in vitro by TNT T7 coupled rabbit reticulocyte lysate system (Promega) at 30°C for 90 min, by following the standard procedure (Huibregtse et al., 1995). After translation, 0.5 μl of peptides in 10% (v/v) DMSO with 10× concentrations shown in Figure 4A were added to the translation reaction mixture (4.5 μL). The resulting mixture was incubated at room temperature at 30 min and

quenched with 2 × SDS-polyacrylamide gel laemli sample buffer (125 mM Tris-HCl [pH 6.8], SDS 4%, glycerol 20%, 0.002% bromophenol blue) in the absence of dithiothreitol. Samples were subjected to SDS-PAGE on a 10% polyacrylamide gel.

In Vitro Polyubiquitination Assay for Prx1 and p53

The plasmid pGEM p53 was used for in vitro translation (Werness et al., 1990). In vitro translation was performed using TNT T7 coupled rabbit reticulocyte lysate system. Recombinant baculovirus for HPV16 E6 was produced using the BaculoGold system (PharMingen) as described previously (Shirakura et al., 2007). Hi5 cells (Invitrogen) were infected with the recombinant baculovirus to produce HPV16 E6 protein. HPV16 E6 Protein was partially purified by anion-exchange chromatography as previously described (Huibregtse et al., 1993). In vitro polyubiquitination assays for Prx1 were performed essentially as described previously (Nasu et al., 2010). Hi5 cells were infected with recombinant baculoviruses AcMEF-E6AP and Ac MEF-E6AP^{C843A} to produce MEF-E6AP and MEF-E6AP^{C843A}, respectively (Shirakura et al., 2007). MEF-E6AP and MEF-E6AP^{C843A} were purified on anti-FLAG M2 agarose beads (Sigma) according to the manufacturer's instructions. Assays were done in 40 μl volumes containing 20 mM Tris (pH 7.6), 50 mM NaCl, 5 mM $MgCl_2$, 100 μM DTT, 5 mM ATP, 250 nM MEF-E6AP or inactive mutant MEF-E6AP^{C843A}, 62.5 nM $(His)_6$-E1, 1.1 μM $(His)_6$-UbcH7, 25 μM ubiquitin, 8 μM $(His)_6$-Prx1 and peptide, and incubation at 37°C for 30 min. Reactions were performed at 37°C for 30 min. The ubiquitination reaction was terminated by freezing the samples with liquid nitrogen. To dissociate proteins, 1% SDS was added to lysates, which were then heated at 90°C for 15 min. The samples were diluted 10-fold with a dissociation dilution buffer containing 1% NP-40, 0.5% deoxycholate, 120 mM NaCl, 50 mM HEPES, 1 mM EDTA, and complete protease inhibitor cocktail (Roche). Samples were immunoprecipitated with anti-Prx1 PAb and analysis by immunoblotting with antiubiquitin mouse monoclonal antibody (anti-Ubi-1, Millipore) to detect ubiquitinated Prx1. In vitro polyubiquitination assays for p53 were performed essentially as described previously (Nakagawa and Huibregtse, 2000). Assays were done in 75 μl volumes containing 25 mM Tris-HCl (pH 8.0), 125 mM NaCl, 2 mM $MgCl_2$, 50 μM DTT, 5 μM ubiquitin, 2 mM ATP, 170 nM MEF-E6AP, 33 nM $(His)_6$-E1, 0.6 μM $(His)_6$-UbcH7, 2 μl of partially purified HPV16 E6, and 5 μl of in vitro translated p53. Peptides inhibitors were added to the samples as indicated. The reaction mixtures were incubated at 37°C for 30 min. The ubiquitination reaction was terminated by freezing the samples with liquid nitrogen. To dissociate proteins, 1% SDS was added to lysates, which were then heated and diluted as described above. Samples were immunoprecipitated with anti-p53 rabbit polyclonal antibody (FL393, Santa Cruz), followed by immunoblotting with antiubiquitin mouse monoclonal antibody (anti-Ubi-1, Millipore) to detect ubiquitinated p53.

SUPPLEMENTAL INFORMATION

Supplemental Information includes four figures, one table, and supplemental Experimental Procedures and may be found with this article online at doi:10.1016/j.chembiol.2011.09.013.

ACKNOWLEDGMENTS

We thank Dr. Hiroshi Murakami for the discussion on conducting this work and Dr. Naoki Goshima for providing the cDNAs of E6AP and Smurf2. This work was supported by the Japan Society for the Promotion of Science (JSPS) Grants-in-Aid for the Specially Promoted Research (Grant 21000005), Research and Development Projects of the Industrial Science and Technology Program in the New Energy and Industrial Technology Development Organization (support to H.S.), Grants-in-Aid for JSPS Fellows (Grant 7734 to Y.Y.), JSPS Grants-in-Aid for Young Scientists (Grant B22710210 to T. Katoh and B22750145 to Y.G.), and Grants-in-Aid for Scientific Research from the Ministry of Health, Labour, and Welfare of Japan (to I.S. and H.S.).

Received: July 13, 2011
Revised: September 20, 2011
Accepted: September 20, 2011
Published: December 22, 2011

REFERENCES

Beaudenon, S., and Huibregtse, J.M. (2008). HPV E6, E6AP and cervical cancer. BMC Biochem. *9* (*Suppl 1*), S4.

Beaudenon, S., Dastur, A., and Huibregtse, J.M. (2005). Expression and assay of HECT domain ligases. Methods Enzymol. *398*, 112–125.

Biron, E., Chatterjee, J., Ovadia, O., Langenegger, D., Brueggen, J., Hoyer, D., Schmid, H.A., Jelinek, R., Gilon, C., Hoffman, A., and Kessler, H. (2008). Improving oral bioavailability of peptides by multiple N-methylation: somatostatin analogues. Angew. Chem. Int. Ed. Engl. *47*, 2595–2599.

Chatterjee, C., Paul, M., Xie, L., and van der Donk, W.A. (2005). Biosynthesis and mode of action of lantibiotics. Chem. Rev. *105*, 633–684.

Chatterjee, J., Gilon, C., Hoffman, A., and Kessler, H. (2008). N-methylation of peptides: a new perspective in medicinal chemistry. Acc. Chem. Res. *41*, 1331–1342.

Doedens, L., Opperer, F., Cai, M., Beck, J.G., Dedek, M., Palmer, E., Hruby, V.J., and Kessler, H. (2010). Multiple N-methylation of MT-II backbone amide bonds leads to melanocortin receptor subtype hMC1R selectivity: pharmacological and conformational studies. J. Am. Chem. Soc. *132*, 8115–8128.

Driggers, E.M., Hale, S.P., Lee, J., and Terrett, N.K. (2008). The exploration of macrocycles for drug discovery—an underexploited structural class. Nat. Rev. Drug Discov. *7*, 608–624.

Eldridge, A.G., and O'Brien, T. (2010). Therapeutic strategies within the ubiquitin proteasome system. Cell Death Differ. *17*, 4–13.

Eletr, Z.M., and Kuhlman, B. (2007). Sequence determinants of E2-E6AP binding affinity and specificity. J. Mol. Biol. *369*, 419–428.

Forster, A.C., Tan, Z., Nalam, M.N., Lin, H., Qu, H., Cornish, V.W., and Blacklow, S.C. (2003). Programming peptidomimetic syntheses by translating genetic codes designed *de novo*. Proc. Natl. Acad. Sci. USA *100*, 6353–6357.

Goto, Y., Ohta, A., Sako, Y., Yamagishi, Y., Murakami, H., and Suga, H. (2008). Reprogramming the translation initiation for the synthesis of physiologically stable cyclic peptides. ACS Chem. Biol. *3*, 120–129.

Goto, Y., Katoh, T., and Suga, H. (2011). Flexizymes for genetic code reprogramming. Nat. Protoc. *6*, 779–790.

Grünewald, J., and Marahiel, M.A. (2006). Chemoenzymatic and template-directed synthesis of bioactive macrocyclic peptides. Microbiol. Mol. Biol. Rev. *70*, 121–146.

Hershko, A., and Ciechanover, A. (1998). The ubiquitin system. Annu. Rev. Biochem. *67*, 425–479.

Hoeller, D., and Dikic, I. (2009). Targeting the ubiquitin system in cancer therapy. Nature *458*, 438–444.

Hoeller, D., Hecker, C.M., and Dikic, I. (2006). Ubiquitin and ubiquitin-like proteins in cancer pathogenesis. Nat. Rev. Cancer *6*, 776–788.

Huang, L., Kinnucan, E., Wang, G., Beaudenon, S., Howley, P.M., Huibregtse, J.M., and Pavletich, N.P. (1999). Structure of an E6AP-UbcH7 complex: insights into ubiquitination by the E2-E3 enzyme cascade. Science *286*, 1321–1326.

Huibregtse, J.M., Scheffner, M., and Howley, P.M. (1991). A cellular protein mediates association of p53 with the E6 oncoprotein of human papillomavirus types 16 or 18. EMBO J. *10*, 4129–4135.

Huibregtse, J.M., Scheffner, M., and Howley, P.M. (1993). Localization of the E6-AP regions that direct human papillomavirus E6 binding, association with p53, and ubiquitination of associated proteins. Mol. Cell. Biol. *13*, 4918–4927.

Huibregtse, J.M., Scheffner, M., Beaudenon, S., and Howley, P.M. (1995). A family of proteins structurally and functionally related to the E6-AP ubiquitin-protein ligase. Proc. Natl. Acad. Sci. USA *92*, 2563–2567.

Josephson, K., Hartman, M.C., and Szostak, J.W. (2005). Ribosomal synthesis of unnatural peptides. J. Am. Chem. Soc. *127*, 11727–11735.

Kawakami, T., Murakami, H., and Suga, H. (2008). Messenger RNA-programmed incorporation of multiple *N*-methyl-amino acids into linear and cyclic peptides. Chem. Biol. *15*, 32–42.

Kohli, R.M., Walsh, C.T., and Burkart, M.D. (2002). Biomimetic synthesis and optimization of cyclic peptide antibiotics. Nature *418*, 658–661.

Kumar, S., Talis, A.L., and Howley, P.M. (1999). Identification of HHR23A as a substrate for E6-associated protein-mediated ubiquitination. J. Biol. Chem. *274*, 18785–18792.

Kung, H.F., Redfield, B., Treadwell, B.V., Eskin, B., Spears, C., and Weissbach, H. (1977). DNA-directed in vitro synthesis of beta-galactosidase: studies with purified factors. J. Biol. Chem. *252*, 6889–6894.

Layfield, R., Lowe, J., and Bedford, L. (2005). The ubiquitin-proteasome system and neurodegenerative disorders. Essays Biochem. *41*, 157–171.

Li, P., and Roller, P.P. (2002). Cyclization strategies in peptide derived drug design. Curr. Top. Med. Chem. *2*, 325–341.

Liu, Y., Cherry, J.J., Dineen, J.V., Androphy, E.J., and Baleja, J.D. (2009). Determinants of stability for the E6 protein of papillomavirus type 16. J. Mol. Biol. *386*, 1123–1137.

Louria-Hayon, I., Alsheich-Bartok, O., Levav-Cohen, Y., Silberman, I., Berger, M., Grossman, T., Matentzoglu, K., Jiang, Y.H., Muller, S., Scheffner, M., et al. (2009). E6AP promotes the degradation of the PML tumor suppressor. Cell Death Differ. *16*, 1156–1166.

McIntosh, J.A., Donia, M.S., and Schmidt, E.W. (2009). Ribosomal peptide natural products: bridging the ribosomal and nonribosomal worlds. Nat. Prod. Rep. *26*, 537–559.

Murakami, H., Ohta, A., Ashigai, H., and Suga, H. (2006). A highly flexible tRNA acylation method for non-natural polypeptide synthesis. Nat. Methods *3*, 357–359.

Nakagawa, S., and Huibregtse, J.M. (2000). Human scribble (Vartul) is targeted for ubiquitin-mediated degradation by the high-risk papillomavirus E6 proteins and the E6AP ubiquitin-protein ligase. Mol. Cell. Biol. *20*, 8244–8253.

Nalepa, G., Rolfe, M., and Harper, J.W. (2006). Drug discovery in the ubiquitin-proteasome system. Nat. Rev. Drug Discov. *5*, 596–613.

Nasu, J., Murakami, K., Miyagawa, S., Yamashita, R., Ichimura, T., Wakita, T., Hotta, H., Miyamura, T., Suzuki, T., Satoh, T., and Shoji, I. (2010). E6AP ubiquitin ligase mediates ubiquitin-dependent degradation of peroxiredoxin 1. J. Cell. Biochem. *111*, 676–685.

Nemoto, N., Miyamoto-Sato, E., Husimi, Y., and Yanagawa, H. (1997). In vitro virus: bonding of mRNA bearing puromycin at the 3′-terminal end to the C-terminal end of its encoded protein on the ribosome *in vitro*. FEBS Lett. *414*, 405–408.

Nestor, J.J., Jr. (2009). The medicinal chemistry of peptides. Curr. Med. Chem. *16*, 4399–4418.

Ogunjimi, A.A., Briant, D.J., Pece-Barbara, N., Le Roy, C., Di Guglielmo, G.M., Kavsak, P., Rasmussen, R.K., Seet, B.T., Sicheri, F., and Wrana, J.L. (2005). Regulation of Smurf2 ubiquitin ligase activity by anchoring the E2 to the HECT domain. Mol. Cell *19*, 297–308.

Ohta, A., Murakami, H., Higashimura, E., and Suga, H. (2007). Synthesis of polyester by means of genetic code reprogramming. Chem. Biol. *14*, 1315–1322.

Ohta, A., Yamagishi, Y., and Suga, H. (2008). Synthesis of biopolymers using genetic code reprogramming. Curr. Opin. Chem. Biol. *12*, 159–167.

Ohuchi, M., Murakami, H., and Suga, H. (2007). The flexizyme system: a highly flexible tRNA aminoacylation tool for the translation apparatus. Curr. Opin. Chem. Biol. *11*, 537–542.

Oman, T.J., and van der Donk, W.A. (2010). Follow the leader: the use of leader peptides to guide natural product biosynthesis. Nat. Chem. Biol. *6*, 9–18.

Pickart, C.M. (2001). Mechanisms underlying ubiquitination. Annu. Rev. Biochem. *70*, 503–533.

Roberts, R.W., and Szostak, J.W. (1997). RNA-peptide fusions for the *in vitro* selection of peptides and proteins. Proc. Natl. Acad. Sci. USA *94*, 12297–12302.

Rubinsztein, D.C. (2006). The roles of intracellular protein-degradation pathways in neurodegeneration. Nature *443*, 780–786.

Sagan, S., Karoyan, P., Lequin, O., Chassaing, G., and Lavielle, S. (2004). N- and Calpha-methylation in biologically active peptides: synthesis, structural and functional aspects. Curr. Med. Chem. *11*, 2799–2822.

Scheffner, M., Werness, B.A., Huibregtse, J.M., Levine, A.J., and Howley, P.M. (1990). The E6 oncoprotein encoded by human papillomavirus types 16 and 18 promotes the degradation of p53. Cell *63*, 1129–1136.

Scheffner, M., Huibregtse, J.M., Vierstra, R.D., and Howley, P.M. (1993). The HPV-16 E6 and E6-AP complex functions as a ubiquitin-protein ligase in the ubiquitination of p53. Cell *75*, 495–505.

Scheffner, M., Nuber, U., and Huibregtse, J.M. (1995). Protein ubiquitination involving an E1-E2-E3 enzyme ubiquitin thioester cascade. Nature *373*, 81–83.

Shimizu, Y., Inoue, A., Tomari, Y., Suzuki, T., Yokogawa, T., Nishikawa, K., and Ueda, T. (2001). Cell-free translation reconstituted with purified components. Nat. Biotechnol. *19*, 751–755.

Shirakura, M., Murakami, K., Ichimura, T., Suzuki, R., Shimoji, T., Fukuda, K., Abe, K., Sato, S., Fukasawa, M., Yamakawa, Y., et al. (2007). E6AP ubiquitin ligase mediates ubiquitylation and degradation of hepatitis C virus core protein. J. Virol. *81*, 1174–1185.

Werness, B.A., Levine, A.J., and Howley, P.M. (1990). Association of human papillomavirus types 16 and 18 E6 proteins with p53. Science *248*, 76–79.

Zhou, P., Lugovskoy, A.A., and Wagner, G.A. (2001). A solubility-enhancement tag (SET) for NMR studies of poorly behaving proteins. J. Biomol. NMR *20*, 11–14.

